Scientia Iranica, Vol. 8, No. 2, pp 92–100
© Sharif University of Technology, April 2001

SCIENTIA
IRANICA

Heat and Mass Transfer in Natural Convection about a Vertical Flat Plate at High Prandtl Numbers

A. Baradaran Rahimi* and S. Gholamdokht[1]

There are many articles in the literature focusing on heat and mass transfer in natural convection considering a vertical flat plate, however, only low Prandtl numbers are usually discussed and not much information exists for the same problem at large Prandtl numbers. In this work, the problem of simultaneous heat and mass transfer in natural convection over an isothermal vertical wall is solved at large Prandtl numbers using perturbation techniques. Starting from Navier-Stokes equations and using similarity transformations, the governing equations are obtained in the form of differential equations. The inverse of Prandtl number is then introduced as the perturbation parameter. The flow is found to have a dual-layer structure. Use of inner and outer expansions leads to uniform values of the relevant quantities. The effects of variation of Prandtl number, Schmidt number, and the ratio of the thermal buoyancy to the total body forces on heat transfer are then investigated.

INTRODUCTION

Circulation of air in atmosphere, water current in oceans, circulation of high Prandtl number fluids used as a heat sink in electrical transformers and, also, flow over a hot wall are all examples of flows dominated by buoyant forces. The simultaneous heat transfer and evaporation of crude oil in different stages of refining process are physical examples of heat and mass transfer. Although current knowledge of simultaneous heat-and-mass transfer problem in natural convection over an isothermal vertical flat plate is extensive, not much information is available when high Prandtl numbers are considered. For example, in 1976, Shenk & Altmann [1] numerically solved problems related to heat and mass transfer in natural convection and illustrated that, in general, heat and mass transfer are functions of the percentage effect of heat transfer buoyancy to the total buoyancy forces. They also showed that at Schmidt numbers close to Prandtl numbers, this dependence becomes weaker. However, their study was limited to low Prandtl numbers, up to $Pr = 0.71$. In other works (e.g., [2,3]) Prandtl numbers as high as $Pr = 7.0$ have been used.

Materials with high Prandtl number are frequently encountered in industry, such as fluids used as heat sink in electrical transformers ($Pr = 47100$ at 273 K), the hydrocarbon polymers or silicons used in some chemical processes and substances such as glycerine ($Pr = 84700$ at 273 K) [4]. Although the above-mentioned numerical research can, in principle, be extended to high Prandtl number fluids, the results are not meaningful because at large Prandtl numbers, the governing differential equations become singular.

In the analysis presented here, Navier-Stokes equations are employed in cartesian coordinates combined with the well-known stream function substitutions of Von Mises and the similarity transformation of Polhausen. The governing equations are, then, obtained in the form of differential equations. Through introducing the inverse of Prandtl number as the perturbation parameter, perturbation techniques are considered for solving this problem. The quantities that change rapidly are analyzed in the thin region near the wall, the so-called inner region, and then are matched with the result in the outer region, avoiding any singularity [5].

In this analysis, it will be shown that: a) in the inner region, buoyancy forces are negligible, b) in the outer region (away from the wall), the inertia forces are

*. *Corresponding Author, Faculty of Engineering, Ferdowsi University of Mashad, P.O. Box 91775-1111, Mashad, I.R. Iran.*

1. *Faculty of Engineering, Ferdowsi University of Mashad, P.O. Box 91775-1111, Mashad, I.R. Iran.*

balanced by friction forces and the buoyancy forces do not exist. Having obtained the governing equations in each region, a shooting method will be used to solve them and at the same time, a matching process will be implemented. The effects of variation of Prandtl and Schmidt numbers and, also, the ratio of the thermal buoyancy to the total body force on heat transfer will be investigated.

FORMULATION OF PROBLEM

The equations to be solved are two-dimensional equations for continuity, momentum and conservation of energy and mass. Neglecting variable property effects other than buoyancy and adapting the well-known boundary layer approximations for steady state conditions, it is obtained that:

$$\frac{\partial u}{\partial x}+\frac{\partial v}{\partial y}=0,$$

$$u\frac{\partial u}{\partial x}+v\frac{\partial u}{\partial y}=g\beta(t-t_\infty)+g\beta^*(\Omega-\Omega_\infty)+\nu\frac{\partial^2 u}{\partial y^2},$$

$$u\frac{\partial t}{\partial x}+v\frac{\partial t}{\partial y}=\alpha\frac{\partial^2 t}{\partial y^2},$$

$$u\frac{\partial \Omega}{\partial x}+v\frac{\partial \Omega}{\partial y}=D\frac{\partial^2 \Omega}{\partial y^2}, \qquad (1)$$

with the following boundary conditions :

$$\begin{aligned} &x>0, \quad y=0, \quad u=v=0, \quad t=t_0, \quad \Omega=\Omega_0,\\ &x>0, \quad y=\infty, \quad u=0, \quad t=0, \quad \Omega=0,\\ &x=0, \quad y>0, \quad u=0, \quad t=0, \quad \Omega=0. \end{aligned} \qquad (2)$$

Here, x and y are vertical and horizontal axes, respectively, as shown in Figure 1. By introducing the stream function substitutions of Von Mises and then the similarity transformation of Polhausen, one gets [6]:

$$f'''-2(f')^2+3ff''+\delta\theta+(1-\delta)\omega=0,$$

$$\theta''+3Pr\ f\theta'=0,$$

$$\omega''+3Scf\omega'=0, \qquad (3)$$

with boundary conditions:

$$\begin{aligned} &\eta=0 \quad \Rightarrow \quad f=f'=0, \quad \theta=1, \quad \omega=1,\\ &\eta\to\infty \quad \Rightarrow \quad f'=0, \quad \theta=0, \quad \omega=0. \end{aligned} \qquad (4)$$

In these formulae, f, θ and ω represent the reduced stream function, temperature and concentration, respectively. The independent variable is $\eta=cyx^{-1/4}$

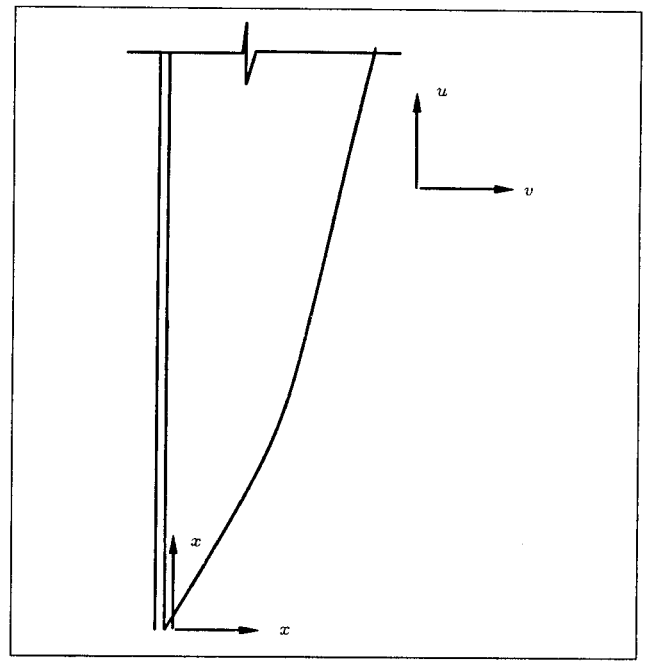

Figure 1. System of coordinates.

(c is a constant which depends on the buoyancy forces). The Prandtl and Schmidt numbers have their usual definition of $Pr=\nu/\alpha$ and $Sc=\nu/D$. The parameter δ represents, essentially, the ratio of the thermal buoyancy to the total body forces and, therefore, $(1-\delta)$ is the ratio of concentration buoyancy to the total effect. For aiding (upward) buoyancy forces, $0<\delta<1$. The mathematical definitions of these quantities are:

$$u=\frac{\partial\psi}{\partial y}=\frac{\nu c^2}{4x}f'(\eta),$$

$$v=-\frac{\partial\psi}{\partial x}=-\nu\left[\frac{\partial c}{\partial x}f(\eta)+\frac{yc^2}{16x^2}f'(\eta)\right],$$

$$\psi(x,y)=c\nu f(\eta),$$

$$c=4\left[\frac{g(\beta\Delta t+\beta^*\Delta\Omega)x^3}{4\nu^2}\right]^{1/4},$$

$$\delta=\frac{\beta\Delta t}{(\beta\Delta t+\beta^*\Delta\Omega)},$$

$$\theta=\frac{t-t_\infty}{\Delta t}, \quad \omega=\frac{\Omega-\Omega_\infty}{\Delta\Omega},$$

where:

$$\Delta t=t_0-t_\infty, \qquad \Delta\Omega=\Omega_0-\Omega_\infty$$

$$\beta=-\frac{1}{\rho}\left(\frac{\partial\rho}{\partial T}\right)_p, \qquad \beta^*=-\frac{1}{\rho}\left(\frac{\partial\rho}{\partial\Omega}\right)_p.$$

PERTURBATION EQUATIONS

Since Prandtl number is high, its inverse, i.e., $\frac{1}{Pr}$, can be used as the perturbation parameter ε. The

governing equations then become:

$$f''' - 2(f')^2 + 3ff'' + \delta\theta + (1-\delta)\omega = 0,$$

$$\varepsilon\theta'' + 3f\theta' = 0,$$

$$\varepsilon\omega'' + 3Le\ f\omega' = 0, \tag{5}$$

where $Le = Sc/Pr$. In the last two equations, ε appears in front of the highest-order terms, thus the problem can be categorized as a "singular perturbation case". Therefore, as $\varepsilon \to 0$, the field must be divided into outer and inner regions, respectively. Obviously, rapid changes take place in the inner region, i.e., near the wall, and results should be matched with the ones obtained for the outer region in order to get uniformly valid solutions throughout the field of study. Next, the governing equations in each of these two regions are determined.

Inner Region

Due to the fact that this is a very thin region near the wall, it is stretched in order to make the quantities of order of one. The stretching variables are:

$$\xi = \frac{\eta}{\varepsilon^{\lambda}}, \quad F(\xi) = \frac{f(\eta)}{\varepsilon^{\gamma}}, \quad \Phi(\xi) = \theta(\eta), \quad W(\xi) = \omega(\eta). \tag{6}$$

Through substituting these variables into Equation 5, collecting terms that are the coefficients of like powers of ε in each equation and taking the limits [5], $\lambda = 1/4$ and $\gamma = 3/4$ are obtained. The governing equations in this region then become:

$$F''' + \varepsilon(-2F'^2 + 3FF'') + \delta\Phi + (1-\delta)W = 0,$$

$$\Phi'' + 3F\Phi' = 0,$$

$$W'' + 3Le\ F\ W' = 0, \tag{7}$$

with the boundary conditions as:

$$\xi = 0, \quad F = F' = 0, \quad \Phi = 1, \quad W = 1. \tag{8}$$

The following perturbation expansions are assumed for the quantities inside the inner region:

$$F(\xi,\varepsilon) = F_0(\xi) + \varepsilon F_1(\xi) + O(\varepsilon^2),$$

$$\Phi(\xi,\varepsilon) = \Phi_0(\xi) + \varepsilon\Phi_1(\xi) + O(\varepsilon^2),$$

$$W(\xi,\varepsilon) = W_0(\xi) + \varepsilon W_1(\xi) + O(\varepsilon^2). \tag{9}$$

Substituting these expansions into the governing equations and collecting the powers of ε and setting their coefficients equal to zero:

ε^0 :

$$F_0''' + \delta\Phi_0 + (1-\delta)W_0 = 0,$$

$$\Phi_0'' + 3F_0\Phi_0' = 0,$$

$$W_0'' + 3Le\ F_0\ W_0' = 0, \tag{10}$$

ε^1 :

$$F_0''' + \delta\Phi_1 + (1-\delta)W_1 = 2F_0'^2 - 3F_0F_0'',$$

$$\Phi_1'' + 3F_0\Phi_1' = -3F_1\Phi_0',$$

$$W_1'' + 3LeF_0W_1' = -3LeF_1w_0', \tag{11}$$

and the corresponding boundary conditions are:

$$F_0(0) = 0, \qquad \Phi_0(0) = 1, \qquad W_0(0) = 1,$$

$$F_1(0) = 0, \qquad \Phi_1(0) = 0, \qquad W_1(0) = 0. \tag{12}$$

Equations 10 to 12 govern the thin region next to the wall, which can be considered a correction factor for the solutions of others.

Outer Region

The changes in this region are gradual, therefore, there is no need for any transformation and Equations 5 govern this region, which is away from the wall. These equations along with the corresponding boundary conditions, are:

$$f''' - 2f'^2 + 3ff'' + \delta\theta + (1-\delta)\omega = 0,$$

$$\varepsilon\theta'' + 3f\theta' = 0,$$

$$\varepsilon\omega'' + 3Le\ f\omega' = 0, \tag{13}$$

$$\eta \to \infty, \quad \theta = 0, \quad \omega = 0, \quad f' = 0. \tag{14}$$

The following perturbation expansions are assumed for the quantities away from the wall:

$$f(\eta,\varepsilon) = f_0(\eta) + \varepsilon f_1(\eta) + O(\varepsilon^2),$$

$$\theta(\eta,\varepsilon) = \theta_0(\eta) + \varepsilon\theta_1(\eta) + O(\varepsilon^2),$$

$$\omega(\eta,\varepsilon) = \omega_0(\eta) + \varepsilon\omega_1(\eta) + O(\varepsilon^2). \tag{15}$$

Substituting these expansions into the above governing equations and collecting the coefficient of like

powers of ε and setting them equal to zero,

ε^0 :

$$f_0''' - 2f_0' + 3f_0 f_0'' = 0$$

$$3f_0\theta_0' = 0$$

$$3Lef_0\omega_0' = 0, \tag{16}$$

ε^1 :

$$f_1''' - 4f_0' f_1' + 3f_0 f_1'' + 3f_1 f_0'' = 0$$

$$3f_0\theta_1' = -3f_1\theta_0' - \theta_0''$$

$$3Lef_0\omega_1' = -3Lef_1\omega_0' - \omega_0''. \tag{17}$$

The boundary conditions are:

$$\eta \to \infty, \quad f_0' = 0, \quad \theta_0 = 0, \quad \omega_0 = 0,$$

$$\eta \to \infty, \quad f_1' = 0, \quad \theta_1 = 0, \quad \omega_1 = 0. \tag{18}$$

These equations are to be solved and matched with the solution of the inner region governing equations. In this process, the unknown integration constants are evaluated.

PERTURBATION SOLUTION

In this section, the solutions of the perturbation equations of Systems 10 and 11, along with the boundary conditions of Equation 12, and the equations of Systems 16 and 17, along with boundary conditions of Equation 18, are presented.

From the second and third equations of Systems 16 and 17, it is seen that $\theta_0(\eta) = 0$, $\theta_1(\eta) = 0$, $\omega_0(\eta) = 0$ and $\omega_1(\eta) = 0$; therefore, in the outer region:

$$\theta(\eta, \varepsilon) = 0,$$

$$\omega(\eta, \varepsilon) = 0. \tag{19}$$

The other two equations of Systems 16 and 17 were solved numerically, along with the equations in Systems 10 and 11, due to their complications. The results were then matched together in order to achieve a uniformly valid solution throughout the region (inner and outer regions). This was done using a general shooting method.

PRESENTATION OF THE RESULTS

System equations 10 and 11 have six equations and six unknowns, which can be solved numerically. These equations constitute the inner solutions which are related to the points very close to the wall. These values are used as boundary conditions for the outer region. Then, the first equations in Systems 16 and 17 are solved using a shooting method. In this manner, the matching process takes place and a uniformly valid solution throughout the region of interest is obtained. In this way, for large values of Prandtl numbers, correct values of quantities are obtained. This procedure can be outlined as follows. Some starting values for unknown quantities are guessed in a middle layer, between the inner and outer regions. These values serve as boundary conditions for inner governing equations and as initial conditions for outer governing equations. A predictor-corrector method [7] is used to shoot the solution of the outer equations to their values at $\eta = \infty$. This is repeated until the best result is obtained. In order to conduct the matching process numerically, in the middle layer, the final inner solutions are set equal to the initial conditions of the outer region equations. The thickness of the inner region is found to be $(O(1/Pr))$ for each case.

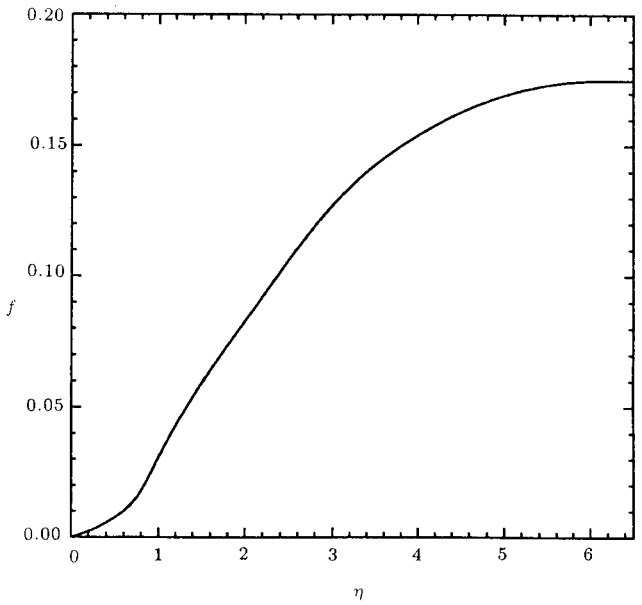

Figure 2. Variation of f versus η for $Pr = 20000$, $Sc = 10$ and $\delta = 0.5$.

Figures 2 to 4 illustrate the matched (uniformly valid) values of the variations of quantities f, θ and ω for different values of Prandtl number. The reduced shear stress, temperature gradient and concentration gradient (f'', θ', ω') are presented in Figures 5 to 7 for different values of Prandtl number. Figures 8 and 9 show the decreasing value of local Nusselt number and increasing value of local Sherwood number against the increasing value of Schmidt number for different values of Prandtl number. Figures 10 and 11 depict the decreasing value of local Nusselt number and decreasing value of local Sherwood number against the increasing value of δ for different values of Prandtl number and $Sc = 10$. In Figures 12 and 13, the increasing value of local Nusselt number and decreasing value of local

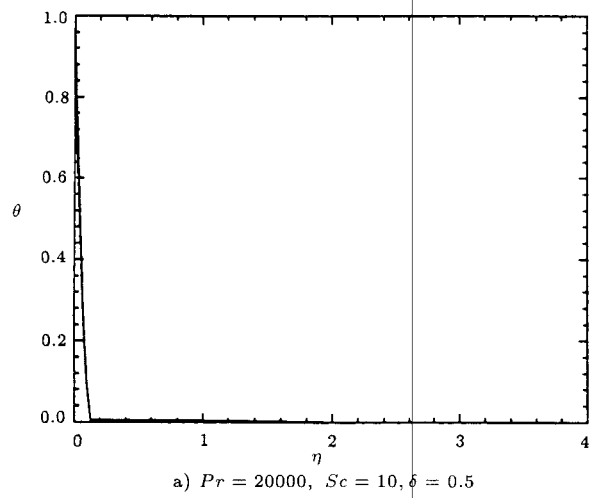

a) $Pr = 20000,\ Sc = 10, \delta = 0.5$

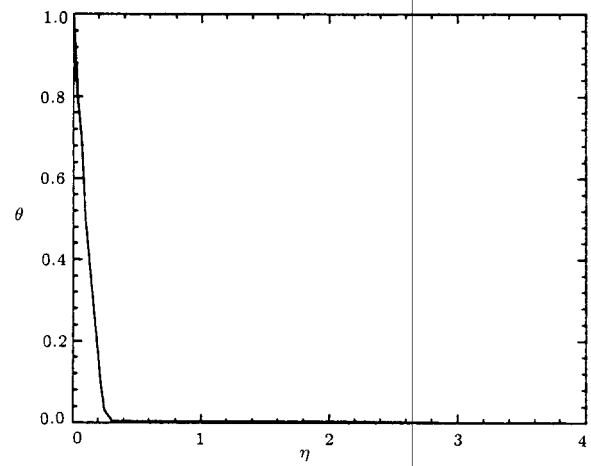

b) $Pr = 1000,\ Sc = 10,\ \delta = 0.5$

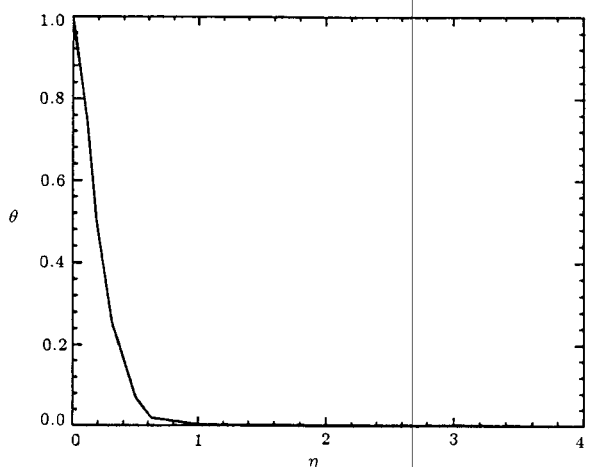

c) $Pr = 100,\ Sc = 10,\ \delta = 0.5$

Figure 3. Variation of θ versus η.

Sherwood number against Prandtl number for $Sc = 10$ and $\delta = 0.5$ are shown. Figure 14 demonstrates the variation of local Nusselt number versus Prandtl number for $Sc = 10$ and $\delta = 1$ (pure heat transfer) along with the result of Ede [8], who has studied natural convection heat transfer in a fluid of high Prandtl number and constant properties.

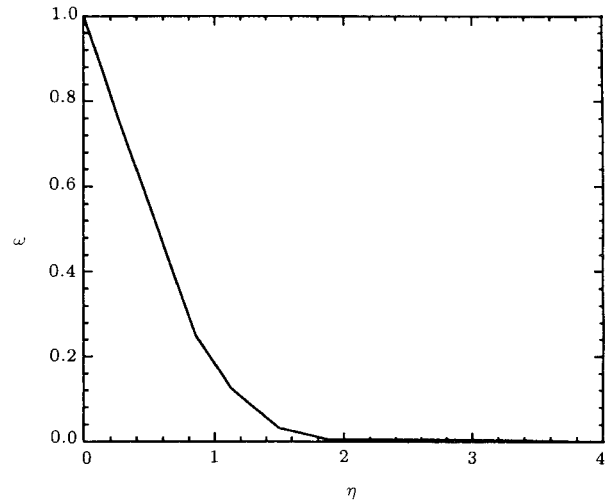

Figure 4. Variation of ω versus η for $Pr = 20000$, $Sc = 10$ and $\delta = 0.5$.

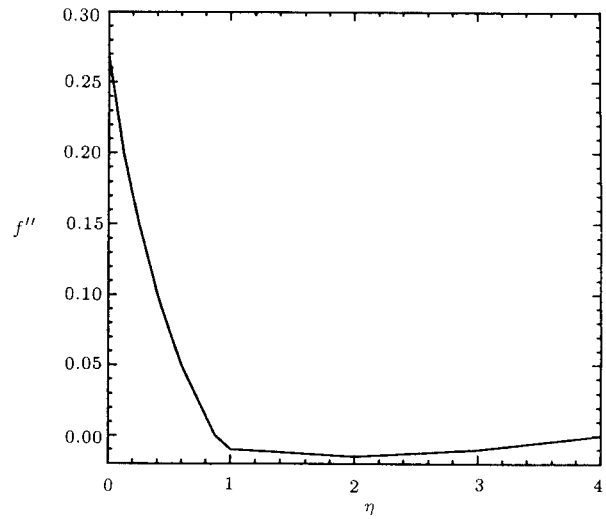

Figure 5. Variation of f' versus η for $Pr = 20000$, $Sc = 10$ and $\delta = 0.5$.

Table 1. Values of $\theta'(0)$ and $\omega'(0)$ versus Pr for $Sc = 10$ and $\delta = 0.5$.

Pr	125	250	500	1000	1500	2000
$-\theta'(0)$	2.85	3.42	4.31	5.51	6.23	7.01
$-\omega'(0)$	1.03	1.018	1.005	0.99	0.982	0.979

In Tables 1 and 2, values of $\theta'(0)$ and $\omega'(0)$ versus Pr and Sc are presented, for example, for $Sc = 10$, $\delta = 0.5$ and $Pr = 1000$, $\delta = 0.5$, respectively.

CONCLUSIONS

In this paper, the influence of mass transfer upon natural convection heat transfer in fluids with high Prandtl number has been determined. The dual-layer structure of the flow permits evaluation of

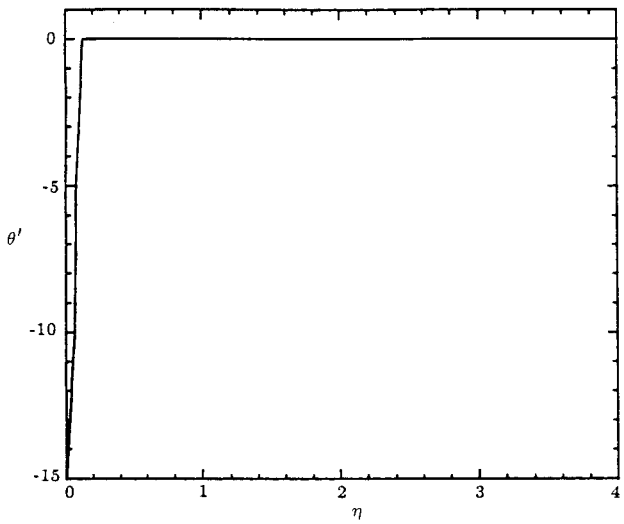

a) $Pr = 20000,\ Sc = 10,\ \delta = 0.5$

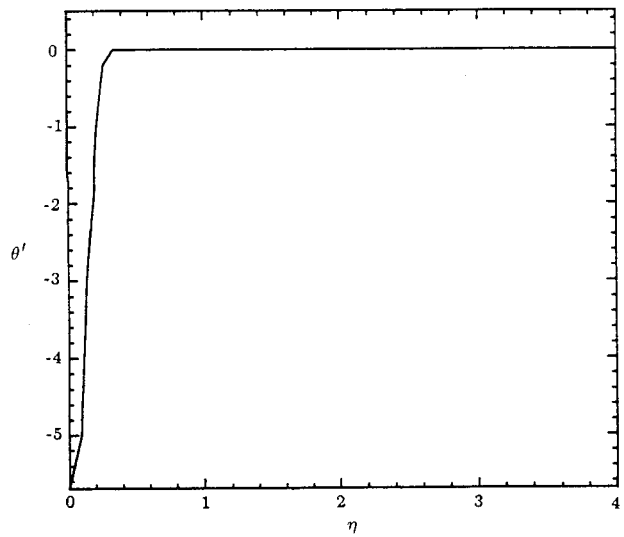

b) $Pr = 1000,\ Sc = 10,\ \delta = 0.5$

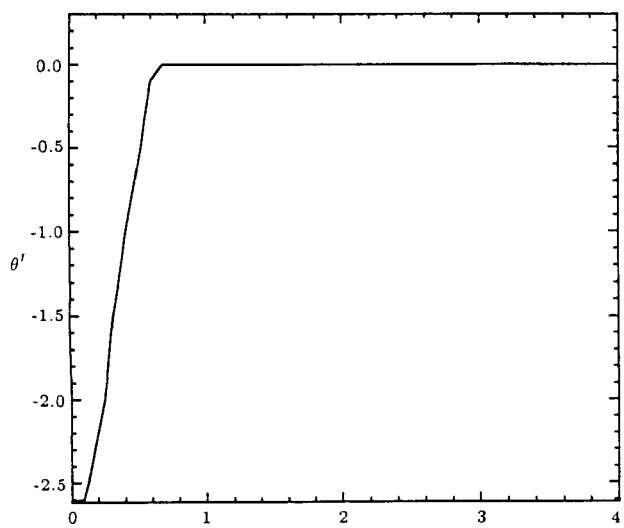

c) $Pr = 100,\ Sc = 10,\ \delta = 0.5$

Figure 6. Variation of θ' versus η.

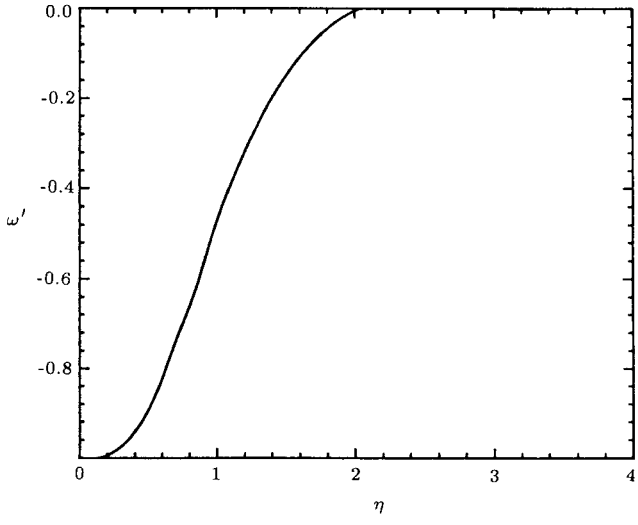

a) $Pr = 20000,\ Sc = 10,\ \delta = 0.5$

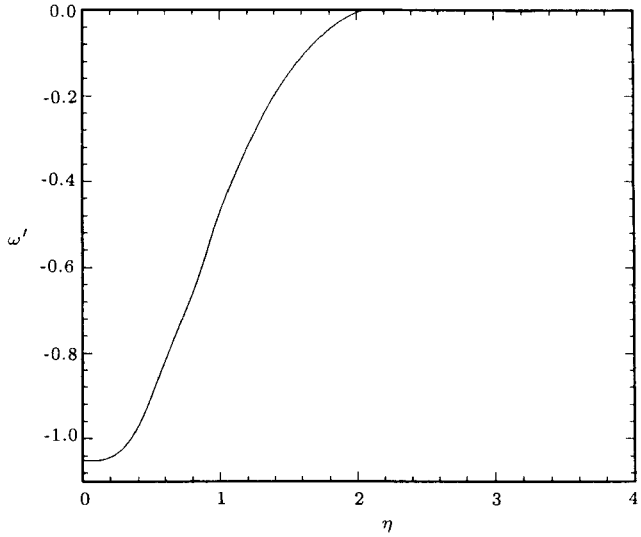

b) $Pr = 1000,\ Sc = 10,\ \delta = 0.5$

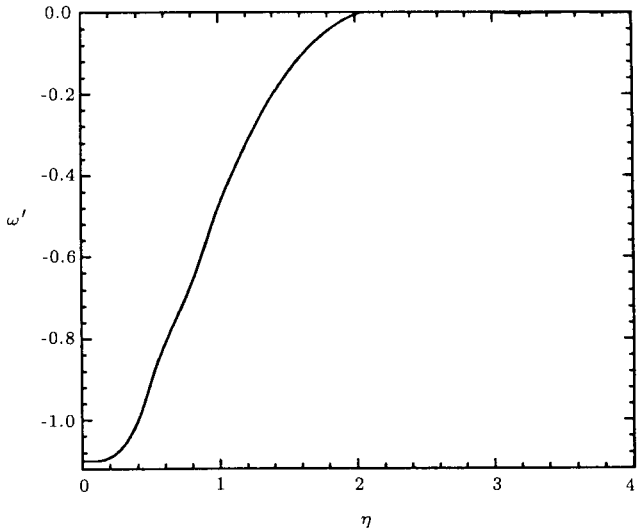

c) $Pr = 100,\ Sc = 10,\ \delta = 0.5$

Figure 7. Variation of ω' versus η.

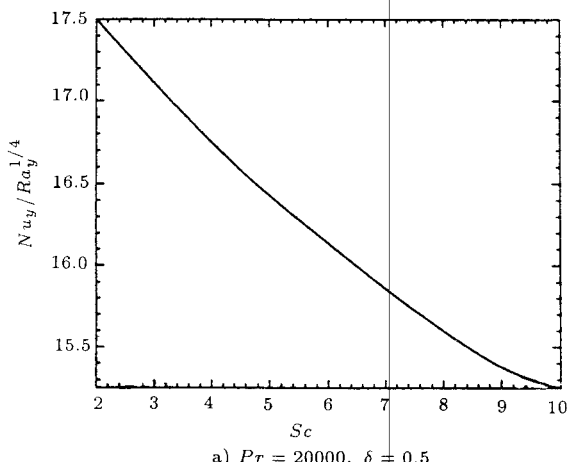

a) $Pr = 20000$, $\delta = 0.5$

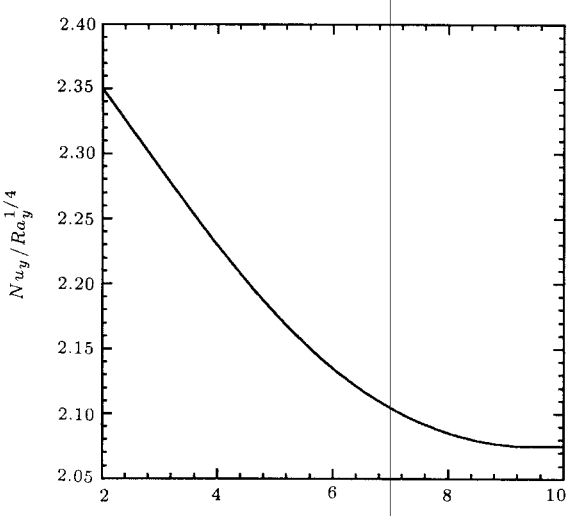

b) $Pr = 1000$, $\delta = 0.5$

Figure 8. Variation of local Nu no. versus Sc no.

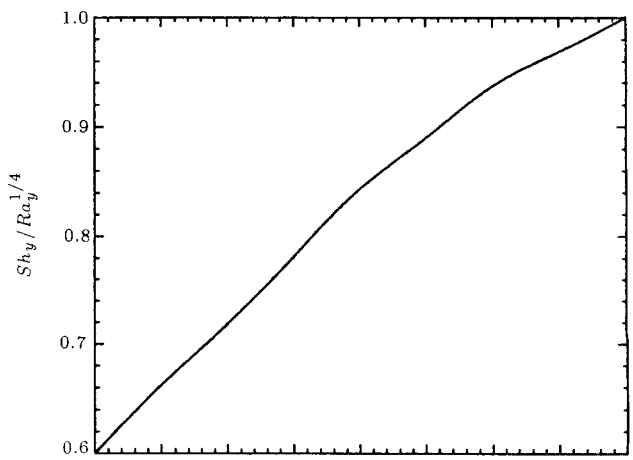

a) $Pr = 20000$, $\delta = 0.5$

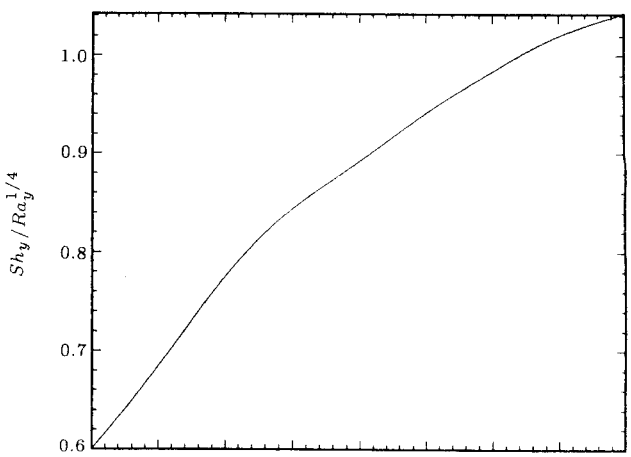

b) $Pr = 1000$, $\delta = 0.5$

Figure 9. Variation of Sh no. versus Sc no.

uniformly valid solution of temperature and concentration throughout the field. Then, the effects of variation of Prandtl number, Schmidt number and the ratio of the thermal buoyancy to the total body forces on heat transfer has been investigated.

In Figures 3a, 3b and 3c, it is observed that an increase in Prandtl number causes temperature variation in the vicinity of the wall to become more rapid. Since fluids with large Prandtl numbers usually have temperature-dependent viscosities [9-11], these results for high Prandtl number might be limited to small temperature differences for high accuracy.

Table 2. Values of $\theta'(0)$ and $\omega'(0)$ versus Sc for $Pr = 1000$ and $\delta = 0.5$.

Sc	2	4	6	7	8	10
$-\theta'(0)$	2.26	2.205	2.12	2.08	2.074	2.05
$-\omega'(0)$	0.685	0.785	0.875	0.93	0.965	1.05

In Figure 14, the result for local Nusselt number in the case of pure heat transfer ($\delta = 1$) is compared with the result presented in [8] which is $Nu = 0.503\ \mathrm{Ra}_y^{1/4}$ converted into the form of similarity transformations. The satisfactory agreement is an evidence of the accuracy of the method presented here.

NOMENCLATURE

Sc	Schmidt number
c	constant
Sh	Sherwood number
D	mass diffusivity
t	temperature
f	reduced stream function
u	velocity component

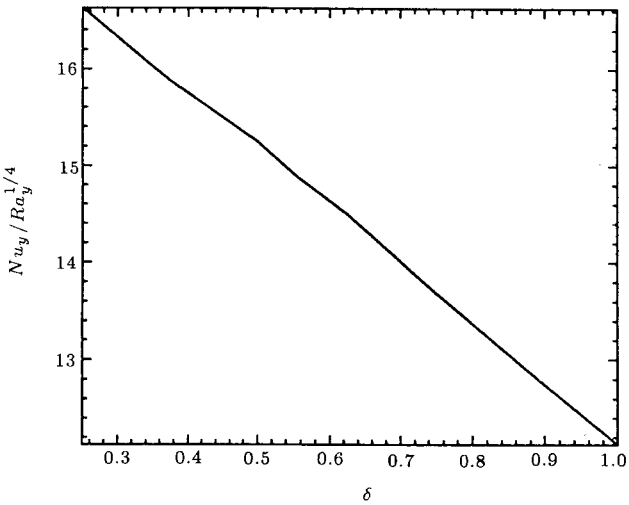

a) $Pr = 20000$, $Sc = 10$

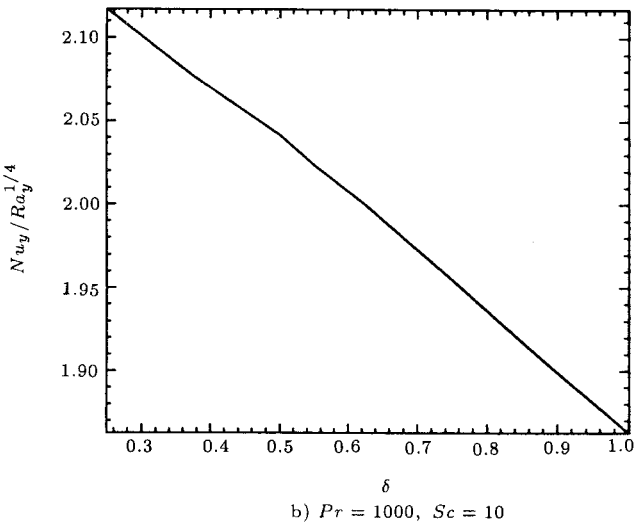

b) $Pr = 1000$, $Sc = 10$

Figure 10. Variation of local Nu no. versus δ.

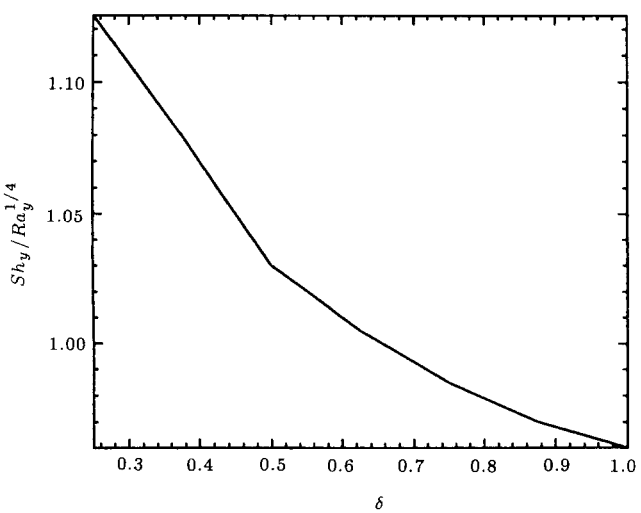

Figure 11. Variation of Sh no. versus δ for $Pr = 20000$ and $Sc = 10$.

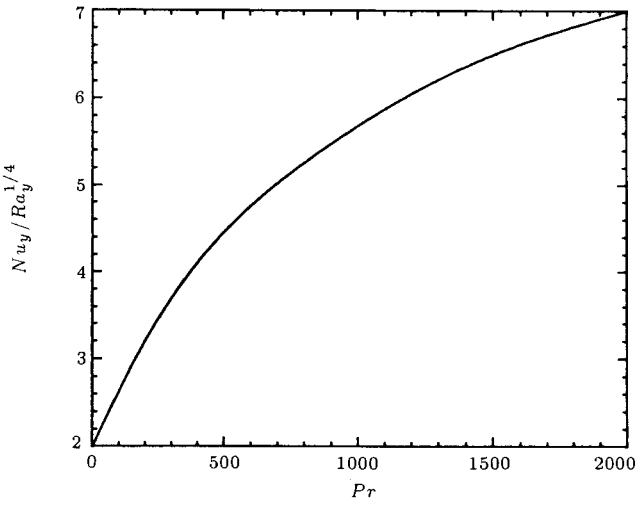

Figure 12. Variation of local Nu no. versus Pr no. for $Sc = 10$ and $\delta = 0.5$.

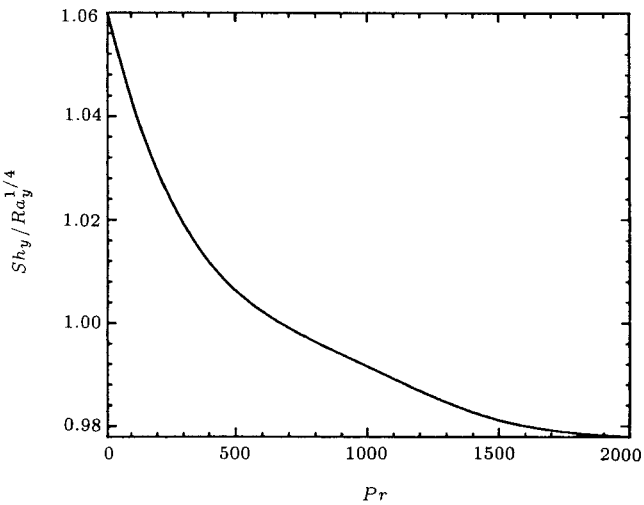

Figure 13. Variation of Sh no. versus Pr no. for $Sc = 10$ and $\delta = 0.5$.

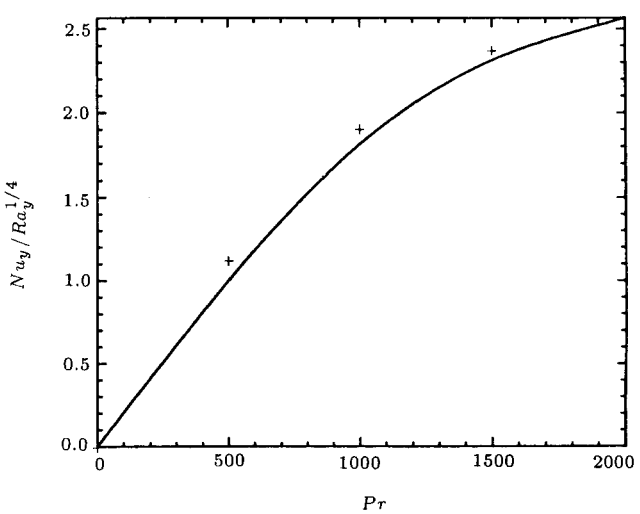

Figure 14. Variation of local Nu no. versus Pr no. for $Sc = 10$ and $\delta = 1.0$ as well as result of [7].

F	stream function in the inner region
v	velocity component
g	gravity acceleration
W	dimensionless concentration in the inner region
Le	Lewis number
Nu	local Nusselt number
x	vertical axis
Pr	Prandtl number
y	horizontal axis
Ra	Rayleigh number

Greek

α	thermal diffusivity
β	$= -\frac{1}{\rho}(\frac{\partial \rho}{\partial T})_p$
β^*	$= -\frac{1}{\rho}(\frac{\partial \rho}{\partial \Omega})_p$
γ	constant
δ	ratio of thermal buoyancy to the total body force
ε	perturbation parameter
η	independent variable in the outer region
λ	constant
θ	dimensionless temperature
ν	kinematic viscosity
ξ	independent variable in the inner region
ρ	density
Φ	temperature in the inner region
ψ	stream function
ω	dimensionless concentration
Ω	concentration

Indices

0	zero-order quantities
1	first-order quantities

REFERENCES

1. Shenk, J. and Altmann, R. "Interaction between heat and mass transfer in simultaneous natural convection about an isothermal vertical flat plate", *Applied Science Research*, **32**, p 599 (1976).
2. Hellums, J.D. and Churchill, S.W. "Transient and steady state free and natural convection, numerical solutions: Part I. The Isothermal vertical plate", *A.I. Ch. E. Journal*, **8**, pp 690-692 (1961).
3. Sammakia, B. and Gebhart, B. "Transient natural convection adjacent to a vertical flat surface: The thermal capacity effect", *Num. Heat Transfer*, **4**, pp 331-344 (1981).
4. Rohsenow, W.H. and Hartnett, J.P. and Ganic, E.N., *Handbook of Heat Transfer Fundamentals*, McGraw-Hill Book Company (1993).
5. Nayfeh, A.H., *Introduction to Perturbation Techniques*, John Wiley (1997).
6. Bottemanne, F.A. "Simultaneous heat transfer and water evaporation by natural convection at a vertical, isothermal surface", *Appl. Sci., Res.*, **25**, p 137 (1972).
7. Press, W.H., Flannery, B.P., Teukolsky, S.A. and Vetterling, W.T., *Numerical Recipes, the Art of Scientific Computing*, Cambridge University Press, Cambridge (1997).
8. Ede, A.J. "Natural convection heat transfer in a fluid of high Prandtl number and constant properties", *Advances in Heat Transfer*, **4**, pp 1-64 (1967).
9. Fujii, T., Takeuchi, M., Fujii, M., Suzaki, K. and Uehera, H. "Experiments on natural convection heat transfer from the outer surface of a vertical cylinder to liquids", *Int. J. Heat and Mass Transfer*, **13**, pp 753-787 (1970).
10. Merkin, J.H. "Mixed convection on a vertical surface with a prescribed heat flux for large Prandtl numbers", *Journal of Mathematical Physics*, **25**, pp 165-190 (1991).
11. Carey, V.P. "Analysis of transient natural convection flow at high Prandtl number using a matched asymptotic expansion technique", *Int. J. Heat and Mass Transfer*, **26**(6), pp 911-919 (1983).